

# On the orbital evolution and growth of protoplanets embedded in a gaseous disc

J.C.B. Papaloizou and J.D. Larwood<sup>★</sup>

*Astronomy Unit, Queen Mary & Westfield College, Mile End Road, London E1 4NS*

Received 1999 November 23.

## ABSTRACT

We present a new computation of the linear tidal interaction of a protoplanetary core with a thin gaseous disc in which it is fully embedded. For the first time a discussion of the orbital evolution of cores on eccentric orbits with eccentricity ( $e$ ) significantly larger than the gas-disc scale height to radius ratio ( $H/r$ ) is given. We find that the direction of orbital migration reverses for  $e > 1.1H/r$ . This occurs as a result of the orbital crossing of resonances in the disc that do not overlap the orbit when the eccentricity is very small. In that case resonances always give a net torque corresponding to inward migration. Simple expressions giving approximate fits to the eccentricity damping rate and the orbital migration rate are presented. We go on to calculate the rate of increase of the mean eccentricity for a system of protoplanetary cores due to dynamical relaxation. By equating the eccentricity damping time-scale with the dynamical relaxation time-scale we deduce that, for parameters thought to be applicable to protoplanetary discs, an equilibrium between eccentricity damping and excitation through scattering is attained on a  $10^3$ – $10^4$  yr time-scale, at 1 au. This equilibrium is maintained during the further migrational and collisional evolution of the system, which occurs on much longer time-scales. The equilibrium thickness of the protoplanet distribution is related to the equilibrium eccentricity and is such that it is generally well confined within the gas disc. By use of a three dimensional direct summation N-body code we simulate the evolution of a system of protoplanetary cores, initialised with a uniform isolation mass of  $0.1M_{\oplus}$ , incorporating our eccentricity damping and migration rates. Assuming that collisions lead to agglomeration, we find that the vertical confinement of the protoplanet distribution permits cores to build up in mass by a factor of  $\sim 10$  in only  $\sim 10^4$  yr, within 1 au. The time-scale required to achieve this is comparable to the migration time-scale. In the context of our model and its particular initial conditions we deduce that it is not possible to build up a massive enough core to form a gas giant planet, before orbital migration ultimately results in the preferential delivery of all such bodies to the neighbourhood of the central star. It remains to be investigated whether different disc models or initial planetesimal distributions might be more favourable for slowing or halting the migration, leading to possible giant planet formation at intermediate radii.

**Key words:** accretion, accretion discs – celestial mechanics, stellar dynamics – Solar system: formation – stars: formation – planetary systems

## 1 INTRODUCTION

The last decade has seen the discovery of Jupiter-sized extrasolar planets orbiting Solar-type stars. In roughly one fifth of the cases recorded to date a planet is inferred to be in nearly circular orbit (having eccentricities less than 0.05) at a distance from the parent star of less than fifteen Solar radii ( $\sim 0.06$  au). In the rest of the detections the planets are inferred to have eccentricities up to 0.7 (with a mean value of 0.3), for semimajor axes in the range 0.07–3 au (Vogt et al. 2000). Thus the orbital characteristics of many of the known extrasolar systems contrast strongly with the gas giants of the Solar system

<sup>★</sup> j.d.larwood@qmw.ac.uk

that have eccentricities less than about 0.05 and semimajor axes greater than 5 au. These new discoveries pose a considerable challenge to the standard models of planetary formation that are based on our knowledge of the Solar system alone.

According to the accumulation model, protoplanetary cores, the building blocks of planet formation, condense from the interstellar dust grains that are initially suspended in the gaseous protostellar disc. These first aggregate to form planetesimals of mass  $10^{18}$ – $10^{20}$  gm (e.g. Weidenschilling & Cuzzi 1993). Seed cores then grow up to an isolation mass, passing through a process of runaway accretion (Lissauer & Stewart 1993). The duration of this growth phase is expected to be on the order of  $10^5$  yr at 1 au (eg. see the reviews by Lin, Bryden, & Ida, 1999, and Papaloizou, Terquem & Nelson, 1999 and references therein). After isolation the orbits of cores do not overlap so that the system evolution slows significantly. Adopting a heavy element surface density of  $6 \text{ gm cm}^{-2}$ , characteristic of the minimum mass Solar nebula, the protoplanetary cores at isolation are thought to have roughly  $0.03M_{\oplus}$  at 1 au from the Sun (Lissauer & Stewart 1993, Lin et al. 1999). For a surface density ten times larger this increases to  $1M_{\oplus}$ .

The cores subsequently interact under their mutual gravitational attraction which can lead to collisions and the consequent production of more massive cores. If a critical mass scale  $\sim 15M_{\oplus}$  can be reached (e.g. Mizuno 1980, Bodenheimer & Pollack 1986), gas accretion can be initiated. Without further growth, the core can build up a substantial gaseous envelope which can contribute much of the final mass of the object as in the case of Jupiter and presumably the giant planets in extrasolar systems. The time-scale for the gas accretion process is estimated to be  $10^6$ – $10^7$  yr (e.g. Bodenheimer & Pollack 1986). A potential problem is that the time required to build up a core with the critical mass may become very long if the cores become isolated and do not migrate (Lissauer & Stewart 1993).

However, in order to discuss the evolution of protoplanetary cores, their gravitational interaction with the gas disc must be taken into account. This interaction produces wave excitation and angular momentum exchange (Lin & Papaloizou 1979) which can lead to orbital migration (Goldreich & Tremaine 1980). Low mass protoplanets interact linearly with the disc and undergo type I inward migration (Ward 1997b). Massive protoplanets interact nonlinearly and undergo type II migration (Lin & Papaloizou 1986). In this paper we shall be concerned with type I migration. In addition to orbital migration, eccentricity damping is produced (Goldreich & Tremaine 1980, Artymowicz 1993, 1994). Normally, migration calculations are undertaken assuming the eccentricity is smaller than the ratio of disc thickness to radius. Since the Solar nebula is generally believed to have been very thin, the latter is a small number, making the small eccentricity assumption very restrictive. Gravitational scattering amongst the cores acts to pump up their eccentricity until damping effects limit it. The possibility that the eccentricity is larger than the ratio of disc thickness to radius should be taken into account. We present here a new computation of the protoplanet-disc interaction in which it is calculated by summing over all resonances required to ensure validity, for eccentricities up to five times the ratio of disc thickness to radius, although in principle any value smaller than unity could be considered.

We use our results to obtain an estimate for the equilibrium values of the mean eccentricity and vertical thickness for a system of protoplanets. This is obtained by balancing pumping through gravitational scattering with damping through tidal interaction with the nebula. The effects of gravitational scattering and the details of the equilibrium are obtained by use of the Boltzmann  $\mathcal{H}$  theorem applied to the Fokker-Planck equation. The limitation of eccentricity because of the protoplanet-disc interaction is manifest in the restricted vertical extent of the protoplanet swarm. That is found to be always well confined within the gaseous disc, which in turn stabilises the collision rate and promotes rapid core agglomeration in comparison to the gas-free case. We investigate the consequences of this through numerical simulations.

In Section 2 we calculate the dynamical relaxation time-scale for a system of equal mass protoplanetary cores by use of the Boltzmann  $\mathcal{H}$  theorem applied to the Fokker Planck equation. In Section 3 we derive the eccentricity damping and orbital migration time-scales in the linear regime for a protoplanetary core that is fully embedded in a thin gaseous disc with surface density  $\propto r^{-1.5}$ . In Section 4 we apply these results to find the vertical extent of a protoplanet swarm at equilibrium as a function of the nebula properties. In Section 5 we present numerical tests of our analysis using a direct summation N-body code in combination with an implementation of our nebula torque model. Specifically, we consider an ensemble of one hundred  $0.1M_{\oplus}$  cores distributed interior to 1 au.

The general finding is that, for characteristic protoplanetary disc parameters, because the eccentricity damping time-scale is significantly shorter than the migration time-scale, a quasi-equilibrium distribution is obtained in a  $10^3$ – $10^4$  yr time-scale at 1 au and which is otherwise proportional to the local disc radius. Inward migration occurs on the much longer migration time-scale and aids the accumulation of up to earth-mass cores in the inner regions of the disc on a  $10^4$ – $10^5$  yr time-scale at  $\sim 1$  au. However, these objects undergo rapid orbital migration towards the central star on the same time-scale, thus in this particular model, gas accretion onto a sufficiently massive core to make a giant planet within the disc lifetime requires a mechanism to halt the migration. One possibility is termination of the disc due to a magnetospheric cavity (Lin, Bodenheimer & Richardson 1996). On the other hand if cores of the same initial mass are formed at much larger radii, they may survive for the disc lifetime without closely approaching the central star. In Section 6 we summarise and discuss these findings. For a first reading of the manuscript we suggest that the general reader moves directly to Section 4.

## 2 ANALYSIS OF GRAVITATIONAL SCATTERING

A system of many bodies interacting under their mutual gravitation can be described by the Fokker-Planck equation which we write in the form:

$$\frac{Df_\alpha}{Dt} = \Gamma_{coll}(f_\alpha) + \Gamma_{gas}(f_\alpha). \quad (1)$$

Here  $f_\alpha$  denotes the phase space number density of bodies with mass  $m_\alpha$ . The operator giving evolution due to gravitational scattering is  $\Gamma_{coll}$ , and that giving evolution due to interaction with the gaseous disc is  $\Gamma_{gas}$ . The latter combines the effects of orbital migration, and eccentricity and inclination damping. The derivative operator is taken following a particle orbit considering gravitational forces due to the central mass such that

$$\frac{D}{Dt} \equiv \frac{\partial}{\partial t} + \mathbf{v} \cdot \frac{\partial}{\partial \mathbf{r}} - \nabla \Phi \cdot \frac{\partial}{\partial \mathbf{v}}. \quad (2)$$

Where we refer to the central potential  $\Phi = -GM_*/r$ , with the particle position and velocity vectors being denoted by  $\mathbf{r}$  and  $\mathbf{v}$  respectively. The central mass is  $M_*$  and  $r = |\mathbf{r}|$ .

## 2.1 Local shearing sheet approximation

As a result of the large relative velocities occurring between objects widely separated in radius, effective gravitational scatterings will occur on a radial length scale comparable to the vertical thickness of the planetesimal disc. The smallness of the latter quantity suggests use of the Goldreich & Lynden-Bell (1964) shearing sheet approximation. In this approximation we consider a uniformly rotating local Cartesian coordinate system in which the origin, located at some point of interest in circular orbit with radius/semimajor axis  $r_0$ , corotates with the Keplerian angular velocity  $\Omega$ . The  $x$ -axis points radially outwards and the  $y$ -axis points in the azimuthal direction while the  $z$ -axis points in the vertical direction. A linear expansion for the central potential is used such that

$$\nabla \Phi = (\Omega^2 r_0 - 2\Omega^2 x, 0, \Omega^2 z). \quad (3)$$

In this scheme we have for an axisymmetric disc with accordingly no dependence on  $y$ ,

$$\frac{Df_\alpha}{Dt} \equiv \frac{\partial f_\alpha}{\partial t} + v_x \frac{\partial f_\alpha}{\partial x} + v_z \frac{\partial f_\alpha}{\partial z} - 2\Omega v_x \frac{\partial f_\alpha}{\partial v_y} + (3\Omega x + 2v_y)\Omega \frac{\partial f_\alpha}{\partial v_x} - \Omega^2 z \frac{\partial f_\alpha}{\partial v_z}, \quad (4)$$

where  $\mathbf{v} = (v_x, v_y, v_z)$  and  $\mathbf{r} = (x, y, z)$ . The Liouville equation  $Df_\alpha/Dt = 0$  has from Jeans' theorem general solutions with  $f_\alpha$  being an arbitrary function of the integrals of the motion. Later we shall adopt such a solution, corresponding to an anisotropic Gaussian:

$$f_\alpha = C_\alpha \exp \left( -\frac{v_x^2}{2\sigma_x^2} - \frac{u_y^2}{2\sigma_y^2} - \frac{v_z^2 + \Omega^2 z^2}{2\sigma_z^2} \right). \quad (5)$$

Here the velocity dispersions  $(\sigma_x, \sigma_y, \sigma_z)$  are constant but such that  $\sigma_y = \sigma_x/2$ . There is no constraint on  $\sigma_z$ . The velocity  $u_y = v_y + 3\Omega x/2$  is measured relative to the local circular velocity,  $v_y = -3\Omega x/2$ , and we shall adopt local relative velocity vectors  $\mathbf{v} = (v_x, u_y, v_z)$ . The constant  $C_\alpha$  is related to the spatial number density in the midplane,  $n_\alpha$ , through

$$C_\alpha = \frac{n_\alpha}{(2\pi)^{3/2} \sigma_x \sigma_y \sigma_z}. \quad (6)$$

## 2.2 System evolution through gravitational scattering

Encounters between planetesimals that occur without direct physical impacts tend to convert kinetic energy from shear into that of random motions, much as viscosity converts energy from shear into thermal motions in a gaseous disc. In the situation considered here evolution due to scattering occurs on a time-scale much longer than orbital. To investigate this phenomenon we use the form of  $\Gamma_{coll}$  given by Binney and Tremaine (1987). This applies to a homogeneous system and so neglects rotation about the central mass. This should be reasonable so long as the time-scale associated with an encounter is short compared to  $\Omega^{-1}$ . This in turn requires that  $\sigma_x/\Omega > r_H$ , where  $r_H$  is the Hill radius  $r_0(\frac{m_\alpha}{3M_*})^{1/3}$ , appropriate to the characteristic mass  $m_\alpha$ .

Following Binney and Tremaine (1987), we write using the summation convention for repeated indices

$$\Gamma_{coll}(f_\alpha) = -\frac{\partial}{\partial v_i} (A_i f_\alpha) + \frac{1}{2} \frac{\partial}{\partial v_i} \left( D_{ij} \frac{\partial f_\alpha}{\partial v_j} \right). \quad (7)$$

Here

$$A_i = 4\pi G^2 \ln(\Lambda) m_\alpha^2 \frac{\partial h}{\partial v_i} \quad (8)$$

and

$$D_{ij} = 4\pi G^2 \ln(\Lambda) m_\alpha^2 \frac{\partial^2 g}{\partial v_i \partial v_j}, \quad (9)$$

with

$$(g, h) = \left( \int f_\alpha(\mathbf{v}') |\mathbf{v} - \mathbf{v}'| d^3\mathbf{v}', \int \frac{f_\alpha(\mathbf{v}')}{|\mathbf{v} - \mathbf{v}'|} d^3\mathbf{v}' \right). \quad (10)$$

For  $\Lambda$  we take  $\Lambda = 3\sigma_x^2 H_\alpha / (4Gm_\alpha)$ , giving the ratio of maximum to minimum impact parameters as disc semi-thickness to impact parameter for a typical deflection (e.g. Binney & Tremaine 1987). The above formalism applies to one species of planetesimal with mass  $m_\alpha$ . Generalization to include a system of interacting planetesimals with different masses is straightforward. However, for simplicity we shall assume all the planetesimals have equal mass in the analysis presented here.

### 2.3 Growth of the velocity dispersion

The effect of gravitational scattering is to cause the velocity dispersion to increase. This is most easily seen by formulating the Boltzmann  $\mathcal{H}$  theorem. This states that for a single mass species

$$\mathcal{H} \equiv - \int f_\alpha \ln(f_\alpha) d^3\mathbf{v} \quad (11)$$

increases monotonically with time.  $\mathcal{H}$ , which can be related to the entropy, can remain constant only for an isotropic Gaussian which cannot be attained here because of the form of particle orbits in the central potential (see equation 5). Using the distribution function given by (5) we obtain at the midplane ( $z = 0$ ), assuming that  $n_\alpha$  is constant and for fixed ratio of velocity dispersion components,

$$\frac{d\mathcal{H}}{dt} = \frac{3n_\alpha}{\sigma_x} \frac{d\sigma_x}{dt}. \quad (12)$$

Thus the velocity dispersion increases with time when  $d\mathcal{H}/dt > 0$ . Here we make the assumption  $n_\alpha$  is constant and specialize to the midplane where  $z = 0$ . We comment that almost identical results are obtained if instead a vertical integration is done and the surface density is assumed constant.

Evaluating  $d\mathcal{H}/dt$ , neglecting for the time being the effects of migration and damping, we obtain using (7):

$$\frac{d\mathcal{H}}{dt} = -4\pi G^2 m_\alpha^2 \ln(\Lambda) \int \frac{\frac{\partial f_\alpha(\mathbf{v})}{\partial v_i} \frac{\partial f_\alpha(\mathbf{v}')}{\partial v'_i}}{|\mathbf{v} - \mathbf{v}'|} d^3\mathbf{v} d^3\mathbf{v}' + 2\pi G^2 m_\alpha^2 \ln(\Lambda) \int \left( \frac{\frac{\partial f_\alpha(\mathbf{v})}{\partial v_i} \frac{\partial f_\alpha(\mathbf{v}')}{\partial v'_j} f_\alpha(\mathbf{v}')}{f_\alpha(\mathbf{v})} \right) \left( \frac{\partial^2 |\mathbf{v} - \mathbf{v}'|}{\partial v_i \partial v_j} \right) d^3\mathbf{v} d^3\mathbf{v}'. \quad (13)$$

Note that the two terms on the right hand side of (13) give contributions of opposite sign. However, a net positive result is guaranteed by the  $\mathcal{H}$  theorem which is why we follow that approach. The integrals in (13) are most easily performed by use of Fourier transforms and the convolution theorem with the result that at  $z = 0$ .

$$\frac{d\mathcal{H}}{dt} = (4\pi)^2 G^2 m_\alpha^2 \ln(\Lambda) (C_\alpha \sigma_x \sigma_y \sigma_z)^2 \int \exp(-k_i^2 \sigma_i^2) \left( \frac{k_i^2}{k^4 \sigma_i^2} - 2 \right) d^3\mathbf{k}. \quad (14)$$

When  $\sigma_y = \sigma_z$ , the integral may be evaluated analytically. Using (12) we then obtain for the relaxation time,  $t_R = \sigma_x / (d\sigma_x/dt)$ ,

$$\frac{1}{t_R} = \frac{8(\pi)^{1/2} G^2 m_\alpha^2 \ln(\Lambda) n_\alpha}{\sigma_x^3} \left[ \frac{\sqrt{3}}{4} \ln \left( \frac{2 + \sqrt{3}}{2 - \sqrt{3}} \right) - 1 \right]. \quad (15)$$

Here we have also specialized to the Keplerian case for which  $\sigma_y = \sigma_x/2$ .

In general the vertical velocity dispersion would be affected by inclination damping. In the case of no damping we expect collisional effects to cause evolution towards isotropy such that  $\sigma_z^2 = (\sigma_x^2 + \sigma_y^2)/2$ , or  $\sigma_z/\sigma_x = 0.79$ . Damping reduces this value, but as long as the rate of inclination damping is comparable to or less than that for eccentricity damping (as is expected to be the case from the results of Ward & Hahn 1994), this effect is not very significant (see below). To obtain a consistent estimate from (15) we adopt the value of  $\sigma_z/\sigma_x = 0.5$ . We shall express the relaxation time in terms of the semi-thickness of the planetesimal disc  $H_\alpha = \sigma_z/\Omega$  and the planetesimal surface density  $\Sigma_\alpha = \sqrt{2\pi} H_\alpha m_\alpha n_\alpha$ . Under these approximations we now have:

$$\Lambda = \left( \frac{3M_*}{m_\alpha} \right) \left( \frac{H_\alpha}{r_0} \right)^3. \quad (16)$$

Thus our analysis is expected to break down when the disc thickness is smaller than the protoplanet Hill radius. Here we obtain:

$$\frac{1}{t_R} = 0.03 \ln(\Lambda) \frac{M_D m_\alpha}{M_*^2} \left( \frac{r_0}{H_\alpha} \right)^4 \Omega, \quad (17)$$

where  $M_D = \pi \Sigma_\alpha r_0^2$  gives an estimate of the protoplanet-disc mass within  $r_0$ . Adopting values consistent with our numerical work:  $M_* = 1M_\odot$ ,  $m_\alpha = 0.1M_\oplus$ ,  $M_D = 10M_\oplus$ , and  $H_\alpha/r_0 = 0.01$ , we find for  $r_0 = 1$  au that  $t_R \sim 3000$  yr. We comment that with  $\sigma_x/\sigma_z = 2$ ,  $H_\alpha/r_0 = 0.01$  corresponds to a mean eccentricity of  $2\sqrt{2}H_\alpha/r_0 \sim 0.03$ .

From this discussion we expect an equilibrium velocity distribution characterized as above, to have been obtained in a time  $\sim 10^3$  yr within 1 au, which is consistent with the numerical results presented below. The actual equilibrium levels of the velocity dispersion are obtained by balancing pumping due to gravitational scattering against damping due to tidal interaction with the nebula. We calculate the latter in the next section.

### 3 TIDAL TORQUES RESULTING FROM NEBULA INTERACTION

Here we calculate the tidal interaction of a protoplanetary core with the gaseous disc. We assume the protoplanet mass is small enough that the disc response is linear. Thus we deal with migration of type I (Ward 1997b).

We employ a simple two dimensional model disc for which the gas surface density  $\sigma \propto r^{-3/2}$ , and the sound speed  $c \propto r^{-1/2}$ . The putative aspect ratio  $H/r$  is thus independent of radius and corotation torques are absent (e.g. Korycansky and Pollack 1993). The gas angular velocity  $\Omega$  is then given by

$$\Omega^2 = \frac{GM_*}{r^3} \left( 1 - \frac{5c^2 r}{2GM_*} \right), \quad (18)$$

and as for Kepler's law this is proportional to  $r^{-3}$ .

The protoplanet or planetesimal of mass  $m_\alpha$  exerts a tidal potential

$$\Psi = - \frac{Gm_\alpha}{\sqrt{r^2 + R^2 - 2rR \cos(\varphi - \varphi_\alpha) + b^2}}, \quad (19)$$

where  $(R, \varphi_\alpha)$  are the cylindrical coordinates of the protoplanet on its general Keplerian orbit. To prevent divergences we incorporate a softening parameter  $b$ . This can be thought of as taking into account the disc vertical thickness.

The protoplanet potential is written as a double Fourier series (e.g. Goldreich and Tremaine 1978) in the form

$$\Psi = \Re \left( \sum_{m=0}^{\infty} \sum_{n=-\infty}^{\infty} \Psi_{n,m} \exp i[(n-m)\omega t + m\varphi] \right). \quad (20)$$

Here  $\Re$  denotes that the real part is to be taken and  $\omega$  is the orbital frequency of the protoplanet taken to have orbital eccentricity  $e$  and semimajor axis  $a \equiv r_0$ . The Fourier coefficients are given by

$$\Psi_{nm} = \frac{\omega}{2\pi^2(1+\delta_{m,0})} \int_0^{2\pi/\omega} \int_0^{2\pi} \Psi \cos[m(\varphi - \varphi_\alpha)] d\varphi \exp[-i(n-m)\omega t - im\varphi_\alpha] dt. \quad (21)$$

Where  $\delta$  is the Kronecker delta. Note that we do not include the indirect term in the above as the contribution due to this is much smaller than that due to terms with large  $m$ . When  $e = 0$ ,  $\Psi_{nm} = 0$  for all  $n \neq 0$ .

In the linear regime the torques due to each Fourier component may be evaluated separately and the results summed. The Fourier component  $(n, m)$  produces a tidal disturbance rotating with a pattern speed  $\Omega_p = (m-n)\omega/m$ . In our model disc only Lindblad resonances are important and if they exist these occur at the two locations in the disc where

$$m^2(\Omega_p - \Omega)^2 = [(m-n)\omega - m\Omega]^2 = \kappa^2 + \frac{c^2 m^2}{r^2}. \quad (22)$$

For  $m > 0$ , the outer Lindblad resonance with  $\Omega < \Omega_p$  occurs where

$$m(\Omega_p - \Omega) = [(m-n)\omega - m\Omega] = \sqrt{\kappa^2 + \frac{c^2 m^2}{r^2}}. \quad (23)$$

The inner Lindblad resonance with  $\Omega > \Omega_p$  occurs where

$$m(\Omega_p - \Omega) = [(m-n)\omega - m\Omega] = -\sqrt{\kappa^2 + \frac{c^2 m^2}{r^2}}. \quad (24)$$

Here the epicyclic frequency  $\kappa = \Omega$ . Note the term  $c^2 m^2 / r^2$ , normally neglected for small  $m$ , leads to an accumulation of resonances at the two locations where  $(\omega - \Omega) = \pm c/r$  as  $m \rightarrow \infty$  for finite  $n$ . These locations are at a distance  $2H/3$  inside and outside the semimajor axis of the orbit. There are no closer resonances for large  $m$ . This leads to the well known torque cut off for  $m \gg r/H$  (Goldreich & Tremaine 1980, Artymowicz 1993) which results in convergence of torque sums in the case of a circular protoplanet orbit ( $n = 0$ ), even when gravitational softening is omitted. However, for general  $n$ , resonances may approach the coorbital radius and so results become more sensitive to the softening parameter. For our disc model the resonant locations occur where

$$\Omega = \frac{(m-n)\omega}{m \pm \sqrt{1 + (H^2 m^2 / r^2)}}. \quad (25)$$

Thus a strictly coorbital resonance occurs if  $n = \pm \sqrt{1 + (H^2 m^2 / r^2)}$ . Even when  $|n| = 1$  two resonances occur at locations satisfying  $(\Omega - \omega) \sim (H/r)\omega$  when  $m \sim r/H$ . These have been found to lead to rapid eccentricity damping (e.g. Artymowicz 1994). Up to now terms with  $|n| > 1$  have not been considered, which is reasonable for very small  $e$ . Here we consider all  $n$  necessary for convergence. Once  $e > H/r$ , significantly larger values of  $n$  are required and these may produce more closely coorbital resonant effects.

We comment that for  $n = 0$ , the inner Lindblad resonances are all located interior to the semimajor axis while the outer Lindblad resonances are all located exterior to it. This results in the inner disc unambiguously providing a positive torque and the outer disc unambiguously providing a negative torque. However, when  $n > 0$ , inner/outer Lindblad resonances may fall

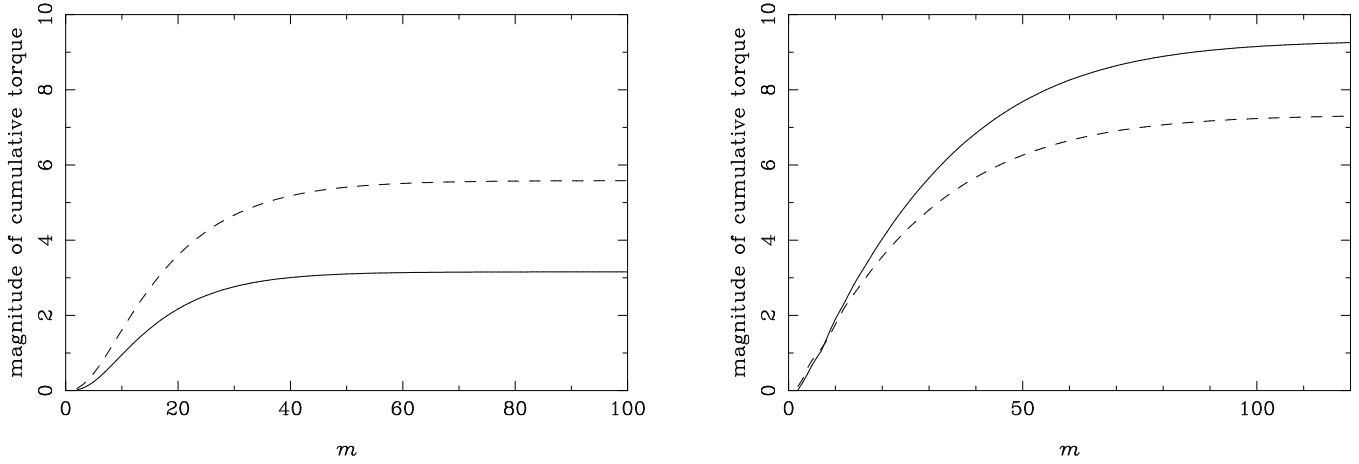


**Figure 1.** The magnitude of the cumulative torque in arbitrary units as a function of  $m$ . The net torque contributions arising from inner Lindblad resonances are plotted with solid lines and those arising from outer Lindblad resonances are plotted with dashed lines. In the left-hand panel we show the magnitudes of the net torque contributions for very small  $e$  and  $H/r = 0.07$ . In this case only  $n = 0$  contributes for each  $m$ . The outer Lindblad resonances predominate leading to net inward migration. In the right-hand panel we show the magnitudes of the net torque contributions for  $e = 2H/r$  and  $H/r = 0.07$ . In this case the torque at each  $m$  has all of the significant contributions from each value of  $n$  included. In this case, unlike when  $e$  is small, the inner Lindblad resonances predominate, leading to net outward migration. Note that these resonances are not all located in the inner disc.

external/internal to the orbital semimajor axis. This means that the interior or exterior discs may produce torques of either sign on an orbit with significant eccentricity. Physically, a protoplanet at apocentre may rotate more slowly than coorbital disc material. If  $e$  is large enough compared to  $H/r$  the exterior disc can then exert a positive torque. We apparently find that this phenomenon may lead to a net torque reversal for sufficiently eccentric orbits.

### 3.1 Rate of orbital evolution

To evaluate the rate of change of protoplanet angular momentum arising from the  $(n, m)$  Fourier component, we use the Goldreich and Tremaine (1978) torque formula as modified by Artymowicz (1993) (see also Ward 1997b) in the form

$$\frac{dJ_{n,m}}{dt} = \frac{Sr^2\Sigma}{3\Omega\Omega_p} \left[ r \frac{d\Psi_{n,m}}{dr} + \frac{2m^2(\Omega - \Omega_p)\Psi_{n,m}}{\Omega} \right]^2 \left[ \frac{1}{1 + 4m^2c^2/(r^2\Omega^2)} \right]. \quad (26)$$

Here  $S = 1$  for an inner Lindblad resonance that transfers angular momentum to the planet,  $S = -1$  for an outer Lindblad resonance that removes it from the planet and the right hand side of (26) is to be evaluated at the resonant location. The associated rate of change of orbital energy is then related to the rate of change of angular momentum through:

$$\frac{dE_{n,m}}{dt} = \Omega_{p,n,m} \frac{dJ_{n,m}}{dt}, \quad (27)$$

where we have added the subscripts  $(n, m)$  to the pattern speed  $\Omega_p$  to denote that it is associated with the corresponding Fourier component.

By summing over  $(n, m)$  we find the total rate of change of angular momentum  $dJ/dt$  and we define the orbital migration time  $t_m$  such that

$$t_m = -\frac{J}{(dJ/dt)}, \quad (28)$$

where  $J$  is the angular momentum of the protoplanet. Migration here is thus defined in terms of the total torque exerted on the orbit. The migration time so defined is positive when the total torque is negative.

Similarly we find the total rate of change of orbital energy and then the rate of change of eccentricity using

$$\frac{1}{J} \left( \frac{dE}{dt} - \omega \frac{dJ}{dt} \right) = \omega \frac{1}{J} \frac{dJ}{dt} \left[ \frac{(1 - \sqrt{1 - e^2})}{\sqrt{1 - e^2}} \right] + \omega \frac{e}{(1 - e^2)^{3/2}} \frac{de}{dt}. \quad (29)$$

The eccentricity evolution time-scale is then

$$t_e = \frac{e}{|de/dt|}. \quad (30)$$

When, as is always found to be the case here,  $de/dt < 0$ ,  $t_e$  gives the circularisation time-scale.

We have performed calculations of  $t_m$  and  $t_e$  taking into account as many resonances as required for convergence. We comment that we did not make any large  $m$  asymptotic approximation as this was found to affect the results significantly.

We illustrate the contributions to the torque for very small  $e$  for which only  $n = 0$  and  $n = 1$  need to be considered in the left-hand panel of Figure 1. The calculation illustrated is for  $H/r = 0.07$ . In this case the contribution from the outer Lindblad resonances that are located in the outer disc dominates and the migration is inwards. The eccentricity is always damped.

We found that departures from the small  $e$  case occurred once  $e > H/r$ . The sign of the torque actually reverses once  $e$  exceeds  $\sim 1.1H/r$ . Significant changes occur because for such values the radial excursion causes the protoplanet to cross the circular orbit resonances a distance  $2H/3$  away from the orbital semimajor axis.

In the right-hand panel of Figure 1 we show the torque contributions from the inner and outer Lindblad resonances for  $H/r = 0.07$  and  $e = 2H/r$ . In this case the inner Lindblad resonances dominate giving a net positive torque. But these are not always located at radii interior to the orbital semimajor axis. The eccentricity is always damped, but note that  $t_e \propto e^3$  for  $e > H/r$ , so that the more eccentric orbits feel very much weaker damping than the near circular ones.

We found that the dependence on the gas-disc thickness was such that  $t_m \propto (H/r_0)^2$ , and  $t_e \propto (H/r_0)^4$ , with  $H$  now being evaluated at  $r = r_0$ . This scaling, together with the coorbital resonance contributions to  $t_e$ , result in  $t_e$  being much shorter than  $t_m$ . Accordingly we expect an equilibrium eccentricity distribution to be set up in a system of gravitationally interacting protoplanets embedded in a gas disc, assuming that they are massive enough so that tidal torques dominate over those due to gas drag. After this equilibrium is set up, longer time-scale evolution is expected to occur due to orbital migration and physical collisions.

We also note that the torque results were dependent on the softening parameter used with  $t_m$  and  $t_e$ , scaling as  $b^{1.75}$  and  $b^{2.5}$  respectively, for  $b$  in the range  $0.4H-H$ . This leads to an uncertainty reflecting the inadequacy of using a two dimensional flat disc model as the softening would occur naturally in a fully three dimensional treatment. Fortunately our simulations of protoplanet discs are insensitive to this issue. Also as we find the eccentricities are for the most part limited to small values, making the results for this case the most important for the work presented here. For small  $e$  our results are broadly consistent with those of Ward (1997b) and Artymowicz (1993, 1994). From our calculations we found the approximate fits to  $t_m$  and  $t_e$  given by

$$t_m = 3.5 \times 10^5 f_s^{1.75} \left[ \frac{1 + \left(\frac{er_0}{1.3H}\right)^5}{1 - \left(\frac{er_0}{1.1H}\right)^4} \right] \left( \frac{H/r_0}{0.07} \right)^2 \left( \frac{2M_J}{M_{GD}} \right) \left( \frac{M_\oplus}{m_\alpha} \right) \left( \frac{r_0}{1 \text{ au}} \right) \text{ yr} \quad (31)$$

and

$$t_e = 2.5 \times 10^3 f_s^{2.5} \left[ 1 + \frac{1}{4} \left( \frac{e}{H/r_0} \right)^3 \right] \left( \frac{H/r_0}{0.07} \right)^4 \left( \frac{2M_J}{M_{GD}} \right) \left( \frac{M_\oplus}{m_\alpha} \right) \left( \frac{r_0}{1 \text{ au}} \right) \text{ yr}. \quad (32)$$

Here the gas disc has a mass  $M_{GD}$  contained within 5 au. At other radii the mass of the gas disc is assumed to scale as  $r_0^{1/2}$ , as implied by the model surface density. The Jovian mass is  $M_J$ . We note that the factor due to softening,  $f_s \equiv \left(\frac{2.5b}{H}\right)$ , is hereinafter taken as unity throughout, corresponding to  $b = 0.4H$ . For  $H = 0.07r_0$ ,  $M_{GD} = 20M_J$ , and  $m_\alpha = 0.1M_\oplus$ , we obtain  $t_e \sim 10^3 \text{ yr}$  and  $t_m \sim 10^5 \text{ yr}$ , in the limit of  $e \ll H/r$  at 1 au.

### 3.2 The contribution from inclination damping

In estimating the damping forces we return to the Boltzmann  $\mathcal{H}$  theorem and consider the contribution to  $d\mathcal{H}/dt$  one obtains from  $\Gamma_{gas}(f_\alpha)$  in equation (1). We suppose this can be represented through the action of a body force  $\mathbf{F}$  per unit mass such that

$$\Gamma_{gas}(f_\alpha) = -\frac{\partial}{\partial \mathbf{v}} (\mathbf{F} f_\alpha). \quad (33)$$

Here if  $\mathbf{F} = -(2v_x/t_e, 0, 2v_z/t_i)$ , the eccentricity and inclination damping times will be  $t_e$  and  $t_i$ , respectively. As migration occurs on a longer time-scale, we shall neglect it when considering the velocity dispersion equilibrium. The damping force  $\mathbf{F}$  gives a contribution to the rate of increase of  $\mathcal{H}$  in the midplane:

$$\frac{d\mathcal{H}}{dt} = -2n_\alpha \left( \frac{1}{t_e} + \frac{1}{t_i} \right). \quad (34)$$

Thus, as long as  $t_i \gtrsim t_e$ , the equilibrium condition  $d\mathcal{H}/dt = 0$  can be approximated by equating  $t_e$  to the relaxation time  $t_R$ , see equation (17).

## 4 VELOCITY DISPERSION EQUILIBRIUM

As we have seen in Section 2, the effect of gravitational scattering not involving direct collisions is to increase velocity dispersion on a time-scale  $t_R$ . An equilibrium is attained by balancing this rate of increase against damping due to tidal interaction of the protoplanet with the gaseous disc. As described in the previous Section we can approximate damping effects by ignoring inclination damping, occurring on the time-scale  $t_i$ , and only consider eccentricity damping, occurring on the time-scale  $t_e$ , provided  $t_e \lesssim t_i$ .

The time-scale  $t_e$  is obtained from the protoplanet-disc interactions calculated above. As this time-scale is significantly

shorter than the migration time-scale  $t_m$ , we expect that a quasi-equilibrium is set up before significant migration occurs and that this then drives the evolution of the system, which will occur under conditions of quasi-equilibrium. To calculate the quasi-equilibrium we use our fit to  $t_e$  given by (32) above and recall our result on the dynamical relaxation time-scale for a central Solar mass point potential:

$$t_R = \frac{5}{\ln(\Lambda)} \frac{M_\odot^2}{M_D m_\alpha} \left( \frac{H_\alpha}{r_0} \right)^4 \left( \frac{r_0}{1 \text{ au}} \right)^{3/2} \text{ yr}, \quad (35)$$

where  $\Lambda$  is given by equation (16). Equating  $t_e$  from equation (32) and  $t_R$ , assuming  $e < H/r_0$  gives the equilibrium semi-thickness of the protoplanet distribution  $H_\alpha$  in terms of the gas disc semi-thickness  $H$ :

$$\frac{H_\alpha}{H} = 0.6[\ln(\Lambda)]^{1/4} \left( \frac{M_D}{M_{GD}} \right)^{1/4} \left( \frac{r_0}{1 \text{ au}} \right)^{-1/8}. \quad (36)$$

$H_\alpha/H$  depends only very weakly on  $\Lambda$  and therefore (36) is essentially independent of the protoplanet mass  $m_\alpha$ , and depends only weakly on other parameters. For  $m_\alpha = 0.1M_\oplus$ , protoplanet disc mass  $M_D = 10M_\oplus$ ,  $H_\alpha/r_0 = 0.01$ , and gas disc mass within 5 au  $M_{GD} = 20M_J$ , we determine  $H_\alpha = 0.15H$  at 1 au. Hence the protoplanet swarm is expected to remain thin and confined within the gaseous nebula. The characteristic eccentricity of the equilibrium (see Section 2) is then roughly  $2\sqrt{2}H_\alpha/r \sim 0.4H/r$ .

## 5 NUMERICAL MODELLING

In order to investigate the consequences of our approximate analysis, we have developed a three dimensional direct summation N-body code to model the gravitational dynamics of a system of protoplanetary cores. For the time integration we employ a fifth order accurate Runge-Kutta-Fehlberg scheme with time step control through the estimated error in velocity magnitude (Press et al. 1992). The scheme is not strictly conservative with the result being orbital decay in the circular orbit two body problem. The accuracy tolerance - used in calculating the computational timestep - was calibrated through experiments with a one Jupiter mass body in circular orbit about the Sun at 0.1 au. We set the accuracy tolerance such that the orbiting body suffered 0.01% orbital decay in  $10^4$  yr, being a much weaker effect than orbital migration due to nebula interaction.

To incorporate the effects of eccentricity and inclination damping and orbital migration owing to tidal interaction with a gaseous disc we implemented the following expressions as contributions to the total acceleration for each particle:

$$\mathbf{a}_{mig} = -\frac{\mathbf{v}}{t_m}, \quad (37)$$

$$\mathbf{a}_{damp} = -2\frac{(\mathbf{v} \cdot \mathbf{r})\mathbf{r}}{r^2 t_e} - 2\frac{(\mathbf{v} \cdot \mathbf{k})\mathbf{k}}{t_i}. \quad (38)$$

Here  $\mathbf{k}$  is the unit vector in the vertical direction. As long as  $t_i$  is not significantly less than  $t_e$ , tests confirm that inclination damping does not change the velocity dispersion equilibrium significantly (see below). Hence the root-mean-square velocity dispersion of the particle distribution is essentially controlled by the quasi-equilibrium eccentricity attained by balancing pumping through gravitational scattering with damping owing to tidal interaction with the gaseous disc.

In all our numerical tests we consider 100 equal mass particles of  $0.1M_\oplus$  each, and a centralised Solar mass. The particle distribution is initialised in the gas-disc midplane such that the surface density is proportional to  $r^{-3/2}$ . The positions are otherwise chosen randomly in the radial range 0.3–1 au such that the separations are greater than twenty Hill radii. The initial velocity components in the midplane correspond to Keplerian circular motion about the central object and vertical velocities are defined as  $iv_\phi$ , where  $i$  is chosen at random for each particle to lie between  $\pm 0.01$ , and  $v_\phi$  is the Keplerian circular velocity.

In a real protostellar accretion disc we expect the mass of the disc at a fixed radius to decrease with time on the global viscous time-scale, which at 1 au is typically  $\sim 10^4$  yr (Papaloizou & Terquem 1999). We note that  $t_e \propto H^4/M_{GD}$  and  $t_m \propto H^2/M_{GD}$ , which tend to increase with diminishing gas-disc mass. However, this increase is compensated for by the decreasing  $H$  found in nebula evolution models (Papaloizou & Terquem 1999). Here we consider a fixed value  $M_{GD} = 20M_J$  which corresponds to an early stage in the life of the nebula at an age  $\sim 10^4$ – $10^5$  yr, in our numerical models. The gas disc then has a mass  $\sim 0.1M_\odot$  within a radius 100 au. However, our calculations of the equilibrium eccentricity distribution (see below) can be scaled to a lower gas-disc mass with smaller vertical scale height by scaling  $H \propto M_{GD}^{1/4}$ . They can also be scaled to apply to larger radii by the scaling transformation:  $(r \rightarrow \lambda r, t \rightarrow \lambda^{1.5} t, M_{GD} \rightarrow M_{GD} \lambda^{-1/2})$ . Thus all radii can be multiplied by 9 provided all times are multiplied by 27 and the disc mass within 5 au is reduced by a factor of 3.

In some of our numerical models we allow the masses to collide and agglomerate. We simulate this process by replacing closely approaching particle pairs with a single mass occupying the centre of mass position of the original pair: the new masses are set up to conserve the mass and linear momentum of the original particle pairs. Binary agglomeration occurs when the separation is less than the sum of the radii associated with each component. For this purpose each mass is assigned a radius that gives a mean density equal to the lunar value. This approach assumes that the relative motion of the colliding pair is completely dissipated and that the liberated kinetic energy does not exceed the total binding energy of the putative bodies. For the relatively large mass scales considered here the latter is expected to be realistic (Lecar & Aarseth 1986). Furthermore, modelling of collisional fragmentation shows that  $> 90\%$  of the total mass remains in the merged core and the existence of

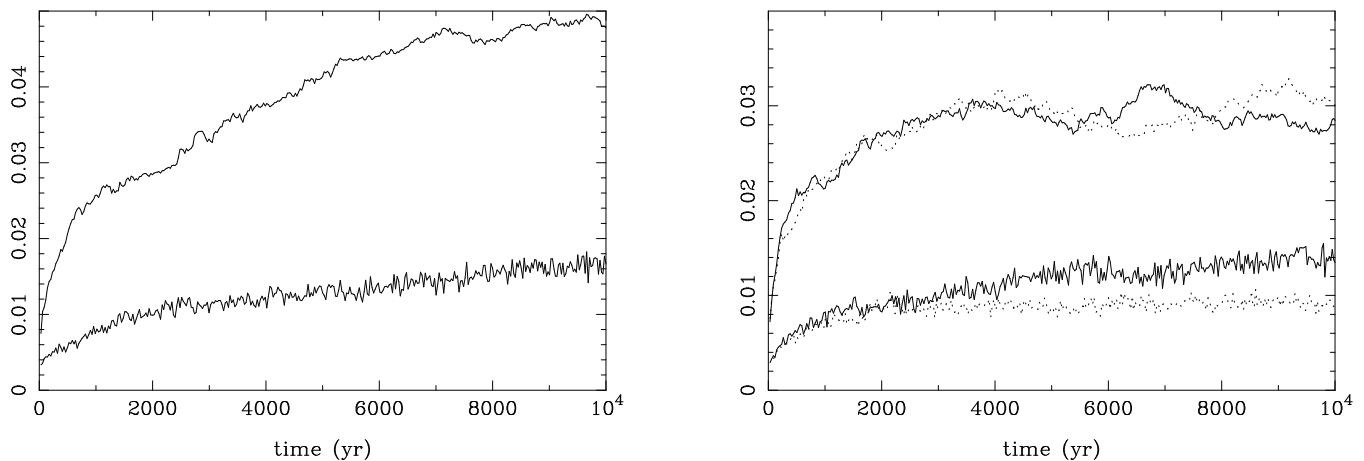


**Figure 2.** Time evolution of the mean eccentricity (uppermost curves) and the mean value of  $|z|/r$  (lowermost curves). The left-hand panel is for a model without nebula torques included in the force calculation. The right-hand panel shows data for a run with eccentricity damping only (solid lines) and a run with both eccentricity damping and inclination damping (dotted lines).

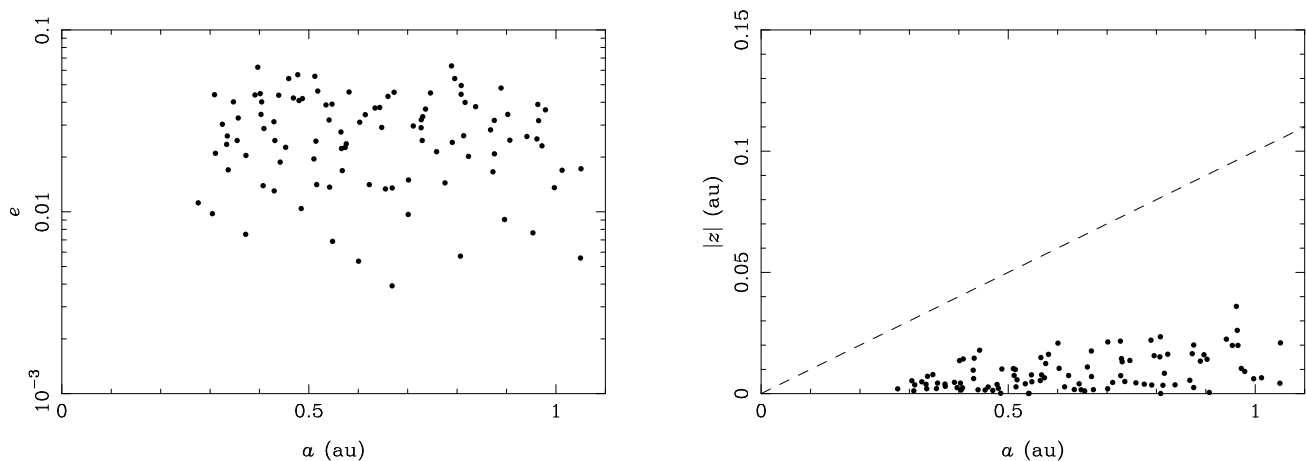


**Figure 3.** The eccentricity and vertical distributions of particles in the model having  $H/r = 0.1$  and no migration or inclination damping, taken at a time of  $10^4$  yr. In the right-hand panel the dashed line refers to the scale height of the putative gas disc.

remnant ejecta is not significant in the subsequent evolution of the planetary system (Alexander & Agnor 1998), and thus can be ignored.

We note that if agglomeration is included in the simulations as described above, and the  $\lambda$  transformation is applied, the physical radius of cores is also scaled. This has the affect that for example if  $\lambda > 1$  the agglomeration time-scale is underestimated. None the less the transformation still serves to indicate how evolutionary time-scales can be increased if initial cores of the same mass are moved to larger radii with a correspondingly reduced disc mass.

### 5.1 Equilibrium eccentricity

In Figure 2 we compare the time evolution of the mean eccentricity and the mean value of  $|z|/r$ , which is used to estimate the characteristic value of  $H_\alpha/r$ . We do this for models with and without damping, but for which we did not include orbital migration or agglomeration. We recall that the dynamical relaxation time-scale estimated above is  $t_R \sim 1400$  yr, at the mean radius. For the model that includes gas with  $H/r = 0.1$  we find  $t_e \sim 6800$  yr, at the mean radius for  $e \ll H/r$  from equation (32).

Without nebula interaction the model cores show eccentricity and vertical thickness increasing monotonically with time. The model that only uses eccentricity damping shows that a quasi-equilibrium in the mean eccentricity is attained after  $\sim 4000$  yr. The average eccentricity is  $\sim 0.3H/r$  and we infer  $H_\alpha/r \sim 0.3H/r$ , broadly in agreement with our analytical estimates outlined in the previous Section.

Comparison of the eccentricity-damped model with a similar model that also includes inclination damping with  $t_i = t_e$  shows that the time-scale and level of the equilibrium eccentricity is essentially the same as before. In the former model, the equilibrium thickness is established after a time  $\sim 4000$  yr. In the latter model, the equilibrium value is established after a time  $\sim 2000$  yr, at a level of about 40% less than for the former model. This value is minimal given the expectation of  $t_i \geq t_e$ .

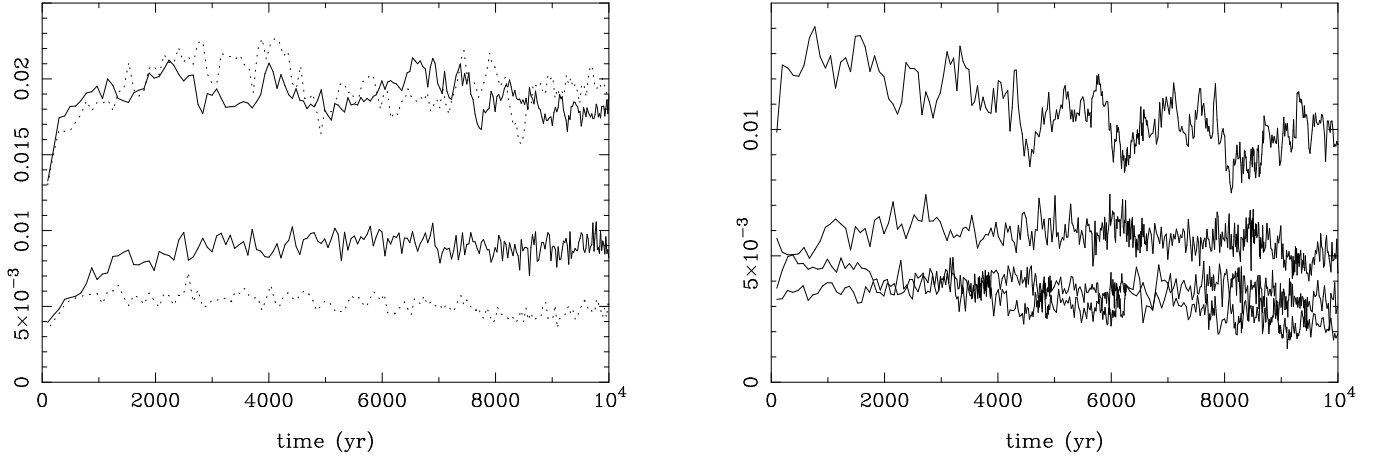


**Figure 4.** Time evolution of the mean eccentricity and the mean value of  $|z|/r$ , for models with damping, migration and agglomeration. The left-hand panel shows data for the  $H/r = 0.07$  runs with eccentricity damping only (solid lines) and with inclination damping included (dotted lines). In both cases the mean eccentricity has the higher value. The right-hand panel shows data for the  $H/r = 0.05$  model (uppermost curves, for which the higher value corresponds to the mean eccentricity), and also the  $H/r = 0.03$  model (lowermost curves, for which the mean eccentricity initially has the higher value).

These calculations assumed  $M_{GD} = 20M_J$ , but can be compared to other gas-disc masses by scaling  $H \propto M_{GD}^{1/4}$ ; for example the minimum mass Solar nebula with  $M_{GD} = 2M_J$  has the same equilibrium as the model used here when  $H/r_0 = 0.06$ . Thus the aspect ratio of the protoplanet swarm relative to the gas-disc aspect ratio increases as the gas-disc mass is reduced.

In Figure 3 we give the eccentricity and vertical position distributions at a time of  $10^4$  yr, for the model without inclination damping. The maximum eccentricity is  $\sim 2/3H/r$ . The low level of eccentricity and inclination in all cases with damping puts the protoplanet distribution well inside the putative disc gas environment, as demonstrated in the right-hand panel of Figure 3. This situation promotes physical collisions in a system of bodies with finite size, which we consider next.

## 5.2 Core agglomeration models

We present models with  $H/r = 0.07$ ,  $0.05$  and  $0.03$ , employing both eccentricity damping and orbital migration. Again,  $M_{GD} = 20M_J$ . For comparison we repeated the model with  $H/r = 0.07$ , but augmented with inclination damping such that  $t_i = t_e$ . Additionally, there is one model without damping or migration. For computational convenience the radius of the central object is taken as  $10R_\odot$  in all cases with orbital migration. First we consider the previously discussed equilibrium in agglomerating simulations, and then protoplanetary growth and orbital migration.

### 5.2.1 Equilibrium

Figure 4 shows the average eccentricity and the mean value of  $|z|/r$  for all our models having migration and damping. The runs with  $H/r = 0.07$  are qualitatively similar to the analogous runs with  $H/r = 0.1$  of the previous Section, with a value of  $\sim 0.3H/r$  for the average eccentricity and  $\sim 0.2H/r$  for the semi-thickness to radius ratio, in the case without inclination damping. Again, inclination damping has little effect on the eccentricity equilibrium, and a moderate effect on the particle-disc thickness, being reduced by  $\sim 40\%$  in this case. The model having intermediate gas-disc thickness  $H/r = 0.05$  gives  $\sim 0.2H/r$  for the average eccentricity, and for  $H_\alpha/r$ , but we note that the averages show a long time-scale decline. This is due to the diminishing particle number, which is a stronger effect in the thinner gas-disc models than for the thicker gas-disc model (see below). We note also that in this model the relative mean eccentricity has dropped in comparison the previous cases, and it is about a half of the predicted value. However, incorporation of migration and agglomeration appears not to strongly affect the establishment of the predicted velocity dispersion equilibrium in these cases.

The thin disc model with  $H/r = 0.03$  shows an equilibrium semi-thickness to radius ratio  $\sim 0.2H/r$ , but the average eccentricity is much smaller than for the thicker disc models at  $\sim 0.1H/r$ , although this has a value  $\sim 0.3H/r$  for the first 2000 yr. In this model the particle-disc thickness is comparable to the mean Hill radius. Consequently the curvature of the Keplerian orbits makes scatterings less efficient at pumping eccentricity than predicted and so the average eccentricity seeks a lower equilibrium value. Hence it is likely that the intermediate gas-disc thickness model is close to being marginally applicable to our analysis, and the agreement on the particle-disc thickness found in the thin gas-disc model is coincidental since the initial mean Hill radius is  $\sim 0.1H/r$ . In our models, in order to compare behaviour at small  $H/r < 0.05$  with the analytical predictions, we would require less massive planetesimals. However, since our analytical results are relatively insensitive to  $m_\alpha$ , similar qualitative behaviour would be expected.

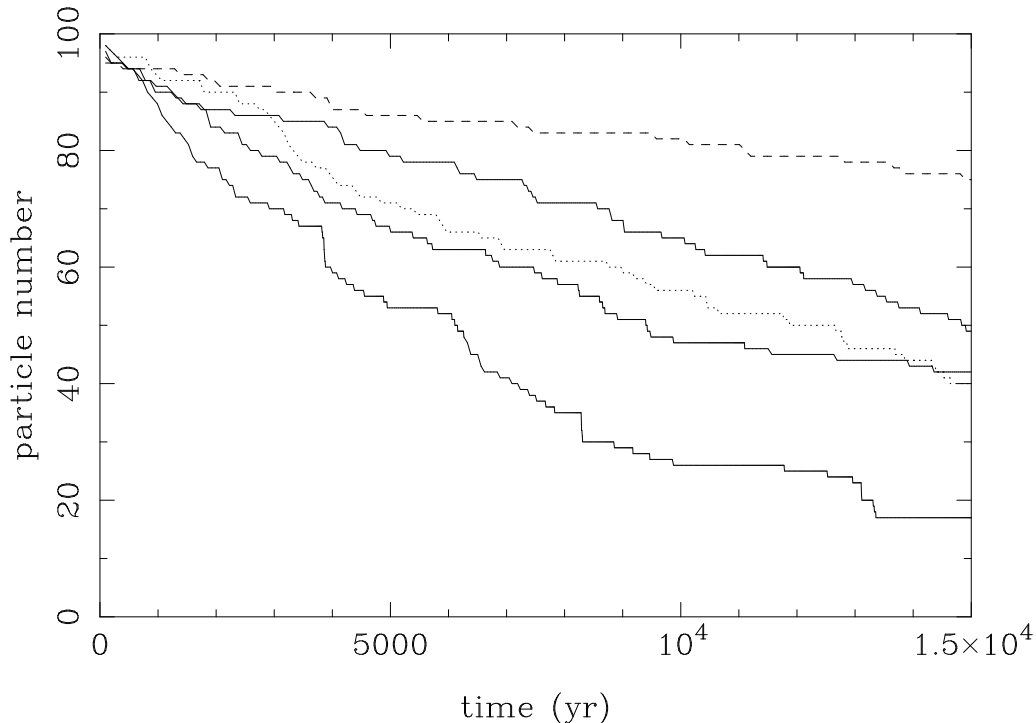


**Figure 5.** The total particle number in the simulations versus time. The data for the model without nebula interaction is plotted with a dashed line, the data for the model with  $H/r = 0.07$  and inclination damping included is plotted with a dotted line. From highest to lowest final value the solid lines are for models with eccentricity damping and orbital migration having  $H/r = 0.07, 0.05, 0.03$ .

### 5.2.2 Protoplanetary growth and orbital migration

In Figure 5 we show the total particle number versus time for models with and without nebula interaction. The former calculations include both damping and orbital migration. The agglomeration time-scale for cores is reduced by including nebula interaction, owing to vertical confinement of the particle distribution, limited radial velocity dispersion and orbit crossing due to migration. The rate of agglomeration for the model with  $t_i = t_e$  and  $H/r = 0.07$  is of similar order to that with  $H/r = 0.05$  and  $t_e$  only, being only about 20% faster than that with  $H/r = 0.07$  and  $t_e$  only. Hence inclination damping does not very significantly enhance the agglomeration time-scale provided  $t_i \gtrsim t_e$ . In all cases with gas-disc models included the accumulation rate is much faster than for the gas-free model. We note that the model with  $H/r = 0.07$  has a migration rate that is comparable to that expected for the minimum mass Solar nebula with  $M_{GD} = 2M_J$  but having  $H/r = 0.02$ .

In Figure 6 we compare the particle trajectories for the models with eccentricity damping and migration only and the case without nebula interaction. In all the cases with nebula interaction included we find that several  $\sim 0.5\text{--}1M_\oplus$  cores build up and undergo increasingly fast migration to the central regions such that the time-scale to build up these masses is comparable to their net migration time-scale. The system thus appears to tend to the situation in which the remaining low mass cores are sufficiently widely spaced that scatterings are no longer effective in raising the eccentricities against damping. However, as long as the core masses are not uniform, differential migration of cores allows further accumulation and rapid migration until uniformity is achieved, or all matter is delivered to the central star. If the former situation occurs, since  $t_m$  increases linearly with radius, there can be no further mass accumulation, as the cores' orbital separations do not decrease with time.

## 6 DISCUSSION

We have derived eccentricity damping and orbital migration time-scales for protoplanetary cores fully embedded in a model gaseous nebula disc with  $\Sigma \propto r^{-1.5}$ . This has been done for  $e$  significantly larger than  $H/r$ , taking into account for the first time all effective contributing resonances  $(n, m)$ . We find that for  $1 > e \gg H/r$  circular orbit calculations are modified in a way indicated by the replacements:  $t_e \rightarrow [e/(H/r)]^3 t_e$  and  $t_m \rightarrow -e/(H/r) t_m$ .

This behaviour is in accord with the simple impulse model for tidal interaction (Lin & Papaloizou 1979). According to this the coupling between the orbit and disc would be expected to be weaker for eccentric orbits owing to the larger relative velocity of the protoplanet and local disc material. The weaker gravitational interaction explains the generally longer time-scales obtained in comparison to the circular orbit case. We also find reversal of the direction of migration, defined according to whether the orbital angular momentum decreases or increases, is possible for sufficiently eccentric orbits ( $e \gtrsim 1.1H/r$ ). This can be thought of as a consequence of the protoplanet spending most time interacting with the disc at apocentre, where the relative velocity of the disc matter gives a predominating contribution to net migration in the outward direction.

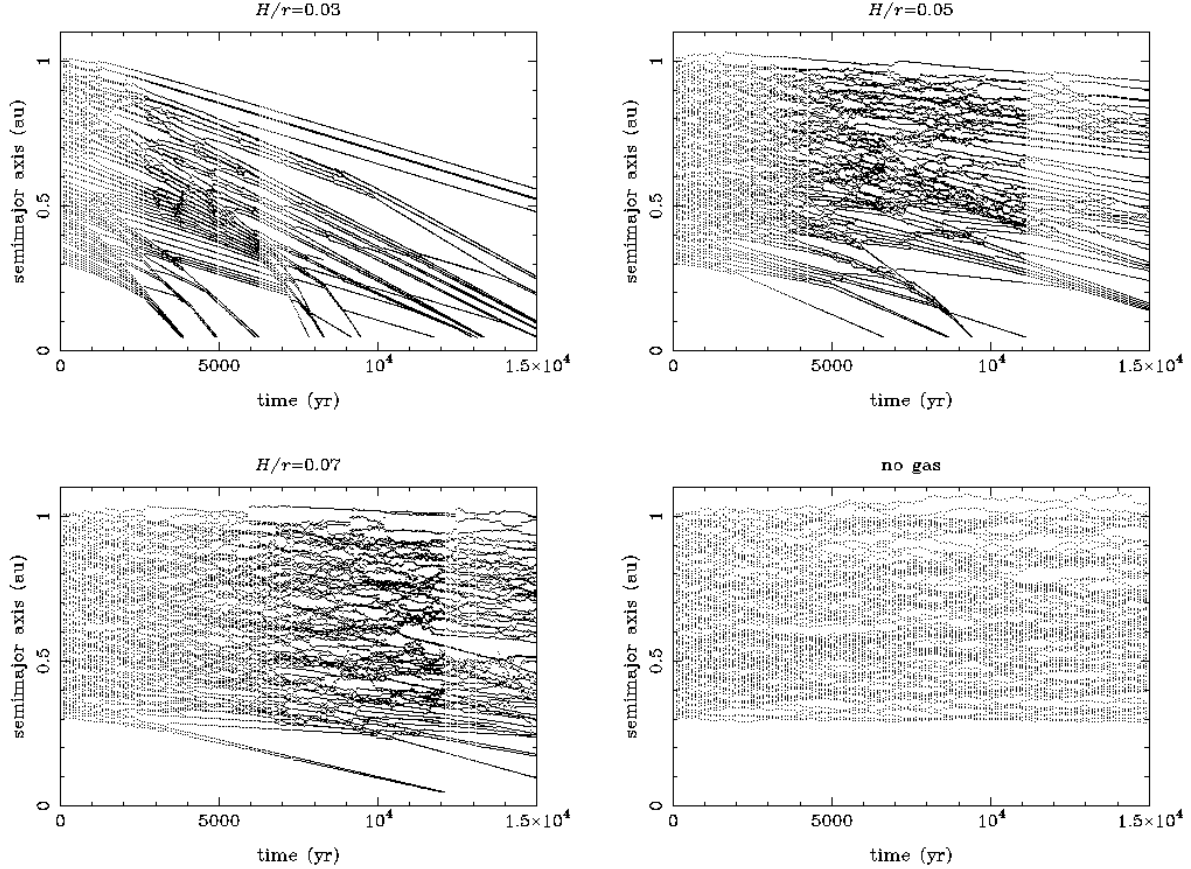


**Figure 6.** Particle semimajor axis versus time for the models without inclination damping, plus the model without nebula torques. Note that the data is not uniformly spaced in time.

We note also that the circularization time-scale can be significantly increased when the orbit has significant eccentricity. Application of (32) indicates that for  $M_{GD} = 2M_J$  and  $H/r = 0.07$ , a critical mass core of  $15M_{\oplus}$  has a circularization time of  $\sim 1.6 \times 10^3$  yr at 10 au. If  $e = 0.35$  this is increased to  $10^5$  yr, which is comparable to the local nebula accretion time-scale. Thus standard inward migration can be prevented if the eccentricity can be maintained against decay by some process such as gravitational interaction with either larger objects and/or a distribution of planetesimals with enough total mass. Accordingly gas accretion onto a critical mass core in an orbit with modest eccentricity should be studied. In this context we note that the notion of a clean annular gap being opened in the disc by the action protoplanetary tides breaks down for eccentric orbits because resonances giving positive and negative torques exist at radii both less than and greater than the semimajor axis. In the small eccentricity case the positive and negative torques are divided separately between the opposing sides of the orbit (Ward 1997b).

We calculated the dynamical relaxation time-scale for a system of cores and deduced the equilibrium eccentricity set up when there is a balance between pumping through gravitational scattering and damping through nebula interaction. We find that the vertical distribution of the protoplanet swarm generally remains well confined within the gaseous envelope of the nebula. This supports our use of a two dimensional analytical model for the tidal interaction.

We determined analytically, and confirmed empirically, that the mean eccentricity and the thickness to radius ratio for the protoplanet swarm are roughly 20–30% of the gas-disc aspect ratio, provided the characteristic size of a protoplanet's Hill sphere is smaller than the latter. But we note that there is a weak dependence on gas-disc and particle-disc mass, and also radius. If the characteristic Hill radius is larger than or comparable to the thickness to radius ratio then lower equilibrium values of thickness and eccentricity occur. The vertical confinement of the cores enhances the collision frequency and consequently promotes more rapid agglomeration into larger objects.

### 6.1 Protoplanetary growth

With the aid of a numerical code we showed that the presence of a gaseous disc can dramatically affect the collisional evolution of a system of gravitating cores. We found that several cores increased in mass by a factor  $\sim 10$  in only  $\sim 10^4$  yr, and underwent

migration to the central star on the same time-scale, for a gas-disc  $\sim 10$  times more massive than the minimum mass Solar nebula. Our scaling for  $t_m$  is such that the migration time-scale for a protoplanet in a  $M_{GD} = 20M_J$  gas disc is the same as for the same protoplanet in the  $M_{GD} = 2M_J$  minimum mass Solar nebula gas disc, but with a moderately reduced  $H/r$ . Additionally, the migration rate of our adopted  $0.1M_{\oplus}$  initial core isolation mass at 1 au scales to the same value for a  $1M_{\oplus}$  protoplanet at 10 au. Starting from an ensemble of equal mass cores embedded in the disc model with  $\Sigma \propto r^{-1.5}$ , as described above, implies that rapid gas accretion onto a massive core cannot occur before it plunges into the star. Tanaka & Ida (1999) reach similar conclusions by considering the growth rate of a migrating  $1M_{\oplus}$  protoplanet through a field of much smaller planetesimals. By extrapolation of the growth rate, they find that for the minimum mass Solar nebula, protoplanets could only build up to a few earth masses before being consumed by the stellar envelope.

Thus the inward migration of at least one core must be halted short of the stellar envelope by some means at the initial stage of clearing, if a gas giant is to be formed at all. If a halting mechanism, such as the presence of a magnetospheric cavity, operates then other cores would be delivered to the first one owing to orbital migration. Providing the migration is not too rapid the inner body could feed on the inflowing objects (Ward 1997a, Papaloizou & Terquem 1999), presumably giving a critical core in only  $\sim 10^4$  yr. But we note that no halting mechanism is known to apply to Jupiter at its present location of 5 au. Although it may be possible that the cores of the outer planets were formed at much larger disc radii with correspondingly longer migration time-scales, and were possibly much closer together in the very early stages of their formation, which could also allow for the mutual excitation of their eccentricities and the consequent stalling of inward orbital migration. It could also be possible that planetesimal scatterings by the cores could help to maintain their eccentricities (Hahn & Malhotra 1999).

Vertical confinement of the protoplanet swarm through inclination damping helps to reduce the agglomeration time-scale without increasing the migration rate. However, for inclination damping time-scales greater than the eccentricity damping time-scale this is not a very significant effect. Even when the zero thickness limit is approached, we still have the problem of type I orbital migration causing very rapid inward migration of the most massive cores.

## ACKNOWLEDGMENTS

This work was supported by PPARC grant GR/H/09454.

## REFERENCES

- Alexander S.G., Agnor C.B., 1998, *Icarus*, 132, 113  
 Artymowicz P., 1993, *ApJ*, 419, 166  
 Artymowicz P., 1994, *ApJ*, 423, 581  
 Binney J., Tremaine S.D., 1987, *Galactic Dynamics* (Princeton University Press, Princeton)  
 Bodenheimer P., Pollack J.B., 1986, *Icarus*, 67, 391  
 Goldreich P., Lynden-Bell D., 1964, *MNRAS*, 130, 125  
 Goldreich P., Tremaine S., 1978, *Icarus*, 34, 227  
 Goldreich P., Tremaine S., 1980, *ApJ*, 241, 425  
 Hahn J.M., Malhotra R., 1999, *AJ*, 117, 3041  
 Korycansky D.G., Pollack J.B., 1993, *Icarus*, 102, 150  
 Lecar M., Aarseth S.J., 1986, *ApJ*, 305, 564  
 Lin D.N.C., Papaloizou J.C.B., 1979, *MNRAS*, 186, 799  
 Lin D.N.C., Papaloizou J.C.B., 1980, *MNRAS*, 191, 37  
 Lin D.N.C., Bryden G., Ida S., 1999, in Sellwood J.A., Goodman J. eds., *Astrophysical Discs - An EC Summer School* (Astronomical Society of the Pacific), p. 207  
 Lissauer J.J., Stewart G.R., 1993, in Levy E.H., Lunine J. eds., *Protostars and Planets III* (Univ. Arizona Press, Tucson), p. 1061  
 Mizuno H., 1980, *Prog. Theor. Phys.*, 64, 544  
 Papaloizou J.C.B., Terquem C., 1999, *MNRAS*, 521, 823  
 Papaloizou J.C.B., Terquem C., Nelson R.P., 1999, in Sellwood J.A., Goodman J. eds., *Astrophysical Discs - An EC Summer School* (Astronomical Society of the Pacific), p. 186  
 Press W.H., Teukolsky S.A., Vetterling W.T., Flannery B.P., 1992, *Numerical Recipes in FORTRAN* (Cambridge Univ. Press, Cambridge), p. 710  
 Tanaka H., Ida S., 1999, *Icarus*, 139, 350  
 Vogt S.S., Marcy G.W., Butler R.P., Apps K., 1999, *ApJ*, submitted  
 Ward W.R., Hahn J.M., 1994, *Icarus*, 110, 95  
 Ward W.R., 1997a, *ApJ*, 482, L211  
 Ward W.R., 1997b, *Icarus*, 126, 261  
 Weidenschilling S.J., Cuzzi J.N., 1993, in Levy E.H., Lunine J. eds., *Protostars and Planets III* (Univ. Arizona Press, Tucson), p. 1031